International Journal of Coal Geology 149 (2015) 118–128

Contents lists available at ScienceDirect

International Journal of Coal Geology

journal homepage: www.elsevier.com/locate/ijcoalgeo

Laboratory investigations of gas flow behaviors in tight anthracite and evaluation of different pulse-decay methods on permeability estimation

Yi Wang, Shimin Liu *, Derek Elsworth

Department of Energy and Mineral Engineering, G3 Center and Energy Institute, Pennsylvania State University, University Park, PA, 16802, USA

ARTICLE INFO

Article history:
Received 18 May 2015
Received in revised form 17 July 2015
Accepted 18 July 2015
Available online 27 July 2015

Keywords:
Permeability evolution in coal
Unconventional gas flow
Ad-/desorption
Pulse-decay method
Uniaxial strain boundary condition
Gas slippage

ABSTRACT

Permeability evolution in coal is critical for the prediction of coalbed methane (CBM) production and CO_2-enhanced-CBM. The anthracite, as the highest rank coal, has ultra-tight structure and the gas flow dynamics is complicated and influenced by multi-mechanistic flow components. Gas transport in anthracite will be a nonlinear multi-mechanistic process also including non-Darcy components like gas as-/desorption, gas slippage and diffusion flow. In this study, a series of laboratory permeability measurements were conducted on an anthracite sample for helium and CO_2 depletions under both constant stress and uniaxial strain boundary conditions. The different transient pulse-decay methods were utilized to estimate the permeability and Klinkenberg correction accounting for slip effect was also used to calculate the intrinsic permeability. The helium permeability results indicate that the overall permeability under uniaxial strain condition is higher than that under constant stress condition because of larger effective stress reduction during gas depletion. At low pressure under constant stress condition, CO_2 permeability enhancement due to sorption-induced matrix shrinkage effect is significant, which can be either clearly observed from the pulse-decay pressure response curves or the data reduced by Cui et al.'s method. But within the same pressure range, there is almost no difference between Brace's method and Dicker & Smits's method. Gas slippage effect is also significant at low pressure for low permeability coal based on the obtained experimental data.

1. Introduction

In the United States, the development of coalbed methane (CBM) was initially encouraged by federal tax incentive during the early 1980s. Since then CBM was considered as a valuable clean energy resource, and the most recent annual energy report by the US Energy Information Administration (Markowski et al., 2014) reveals an incredible increment in coalbed methane production from 1989 to 2008 (Fig. 1). Although after 2009 the production rate shows a little decline trend, CBM is still an important natural gas production contributor. In the US, Pennsylvania is the fourth largest coal producing state in the nation in 2014 and the only state producing anthracite coal. Anthracite coal has a general higher heating value than other coal types (Coal Age, 2014). The anthracites were known as ultra-tight and also the highest rank coal with the highest fixed carbon content. Additionally, from an environmental standpoint, CO_2 sequestration in anthracite coal seams is also attractive due to the high CO_2 holding capacity per unit volume/mass. For both anthracite-CBM and CO_2-enhanced CBM, the permeability of coal is one of the key decision-making parameters and thus a sound knowledge of the permeability evolution for anthracites will be essential.

During CBM production, the permeability of coal dynamically changes as a result of pressure drawdown. When pressure decreases, there will be an increase of the effective stress, defined as the difference between the external stress and pore pressure, tending to close the aperture of existing fractures (Cui and Bustin, 2005; Mazumder and Wolf, 2008; Palmer and Mansoori, 1998; Shi and Durucan, 2004; Wang et al., 2012a; Wang et al., 2012b; Wang et al., 2011). And the pressure drawdown also results in coal matrix shrinkage through a thermodynamic energy balance which tends to open the factures and an enhancement of permeability (Liu and Harpalani, 2013a, 2013b; Pan and Connell, 2007). The permeability evolution is, therefore, controlled by two competitive effects, namely, stress induced permeability reduction and matrix shrinkage induced permeability enhancement during pressure depletion. What's more, gas flow in anthracites is expected to be influenced by multi-mechanistic flow dynamics such as sorption, diffusion, slippage and, Darcy flows (Javadpour, 2009). The non-Darcy flows could be significant in anthracites because of the extremely tight matrix structure when the mean gas flow path is comparable with the pore size. Thus, the estimated permeability by assuming only Darcy's flow may not be valid for tight anthracites with non-ideal gases like N_2, methane and CO_2 (Gensterblum et al., 2014), and the characterization of non-Darcy components raises its importance for both laboratory measurements and modeling.

In this paper, the transient method “pulse-decay” technique was used to measure the low permeability on anthracite sample (Brace

* Corresponding author.
E-mail address: szl3@psu.edu (S. Liu).

http://dx.doi.org/10.1016/j.coal.2015.07.009
0166-5162/

et al., 1968). However, this original pulse-decay method has its limitations when applying to coal or other organic-rich reservoir rocks. For example, it assumes no compressive storage in the rock sample (Hsieh et al., 1981), pure Darcy's flow components without sorption effect (Cui et al., 2009) and no gas slippage effect (Heller et al., 2014). Thus in this study, both pulse-decay approaches with pore compressive storage effect developed by (Dicker and Smits, 1988) and with sorption effect developed by (Cui et al., 2009) will be employed along with the classic pulse-decay and Klinkenberg correction will be introduced to weigh the contribution of slip flow, in order to test how non-Darcy effect would impact the tight coal permeability. Also, the permeability was measured under various experimental boundary conditions and the influence of different boundaries was discussed in detail.

2. Background and literature review

2.1. Anthracite-CBM studies

Coal is generally considered as a self-source reservoir rock with high gas storage capacity due to sorption effect. Anthracite, as the highest rank coal, has higher adsorption capacity for gas storage than lower rank coals (Markowski, 2014). However, anthracite coal has a relatively low porosity due to high thermal maturity. Thus the lessons learned from fluid dynamics in tight-shale may help us to better understand the permeability evolution of anthracite coal. The past coal permeability studies on anthracites showed complex permeability behaviors with combined matrix swelling/shrinking and effective stresses effects (Izadi et al., 2011; Wang et al., 2011; Yin et al., 2013). Also, gas transport in anthracites is a multi-mechanistic process including sorption, diffusion, slip and advection flows. Therefore, a comprehensive characterization and evaluation of anthracite coal permeability evolution in laboratory scale is critical to decipher the complexity of gas and coal interactions during CBM/ECBM production.

2.2. Compressive storage and sorption effect on coal permeability

Compressive storage of the reservoir in pulse-decay permeability measurements is influenced by instantaneous volumetric flow rate change, pressure drop rate and fluid and reservoir compressibility (Jones, 1997). The original pulse-decay developed by Brace et al. (1968) assumed no compressive storage effect in rock sample. Hsieh et al. (1981) then derived a general solution accounting for the compressive storage effect in pulse-decay, and Dicker and Smits (1988) presented a new model to apply this effect into pulse-decay method. The significance of this effect depends on the ratio between the compressive storage inside the sample and in the up-/downstream reservoirs, which means it needs to be evaluated case by case. Since both Brace's method and Dicker & Smits's method have been widely applied in sample permeability measurements, the feasibility of each method, in our case, should be deliberately tested for ultra-tight rocks.

As a primary storage mechanism in CBM reservoirs, adsorption is, especially, necessary for indirect gas content estimation (Hartman, 2008). Gas sorption capacity is typically influenced by pressure, temperature, microstructure of the rock, and it is further found that the absorbed amount of gas is proportional to the organic carbon content of the rock (Hildenbrand et al., 2006; Pillalamarry et al., 2011; Walls et al., 2012; Zhang et al., 2012). For coals, adsorption has indirect influence on gas transport properties (Cui et al., 2009). Permeability is a factor measuring the ability of fluid flow through a porous medium following Darcy's law (Mckernan et al., 2014). During CBM production, methane molecules desorb from the internal surfaces of matrix resulting a matrix shrinkage that opens natural cleats and then increase of permeability (Liu and Harpalani, 2014a; Mitra et al., 2012). In (Liu and Harpalani, 2013a), both mechanical effect and sorption induced strain during reservoir depletion was combined in a sorption-induced strain model that can be coupled into existing permeability models (Liu and Harpalani, 2013b). This coupled model was tested to be valid for subbituminous coal. However, the roles of sorption effect on the high rank anthracite permeability has not been investigate and quantified.

2.3. Pulse-decay method for stressed rock permeability estimation

Significant experimental work has been tried to measure the permeability and its evolution in coal and other tight rocks. Brace et al. (Brace et al., 1968) firstly introduced the pulse-decay technique as a transient method derived from Darcy's law to simply measure the permeability by applying a pressure difference between two sides of a core sample. After the initial pulse-decay method was introduced, this technique has been extensively applied for the tight rock permeability estimation. Different data interpretation methods were used by different scholars and they were summarized in Table 1 (Cui et al., 2009; Dicker and Smits, 1988; Jones, 1997; Kamath et al., 1992; Luffel et al., 1993; Malkovsky et al., 2009; Wang et al., 2011). Dicker and Smits (1988) proposed a pulse-decay calculation method with pore volume compressive storage effect correction. However, they didn't incorporate any adsorption effect and non-Darcy flow regimes into the calculation to be suitable for the unconventional gas permeability measurements. Moreover, laboratory estimation of permeability of unconventional reservoir rocks with adsorption effect has been reported and it has been traditionally measured either under hydrostatic conditions (Cui et al., 2009; Soeder, 1988) or in the absence of applied stress (Cui et al., 2009). In (Cui and Bustin, 2005), an approach was proposed to explicitly include adsorption during pulse-decay method to measure the rock sample permeability. A sorption capacity term firstly derived by Dicker and Smits (1988) was implicitly introduced to correct the compressive storage in pore space at different pressures. Wang et al. (2011) used the original pulse-decay calculation method to measure the coal permeability and to quantify the sorption amount and sorption-induced strain under fixed stressed condition. These laboratory work advanced the understandings of the unconventional gas permeability measurements, but their laboratory conditions are not representative of true field conditions and consequently, the findings may be subject to faulty permeability measurements of sorptive-elastic media (Liu and Harpalani, 2014a, 2014b; Mitra et al., 2012).

Mitra et al. (2012) presented a step-wise laboratory permeability experiment under uniaxial condition, which replicates in situ condition of reservoir by fixing the lateral dimension and vertical stress. The application of uniaxial strain condition can interpret the dynamic changes of the state of stress during reservoir depletion (Liu and Harpalani, 2014c; Shi and Durucan, 2014; Shi et al., 2014). The uniaxial strain condition is widely accepted as in situ condition for subsurface reservoir development, in which the lateral boundaries of a reservoir are fixed and do not move, as well as the constant vertical stress due to the unchanged overburden (Geertsma, 1966; Lorenz et al., 1991). A reduction in reservoir pressure, in turn, results in a reduction in stress acting within and surrounding the reservoir. The horizontal stress acting in a reservoir at depth is observed to decrease significantly with decreasing reservoir pore pressure (Liu and Harpalani, 2014c). This stress decrease is known from simple theoretical calculations and has been observed in field for many conventional reservoir formations (Breckels and Eekelen, 1982; Teufel et al., 1991). In this study, permeability measurements were conducted on tight anthracite coal samples and different pulse-decay approaches were applied to figure out the feasibility of each method on unconventional reservoir rocks, with the evaluation of the permeability data under both constant stress condition and uniaxial strain condition.

2.4. Slip effect

Note that unconventional reservoir rock has very tight structure, gas flow in matrix is controlled by multiple flow dynamics including Darcy's

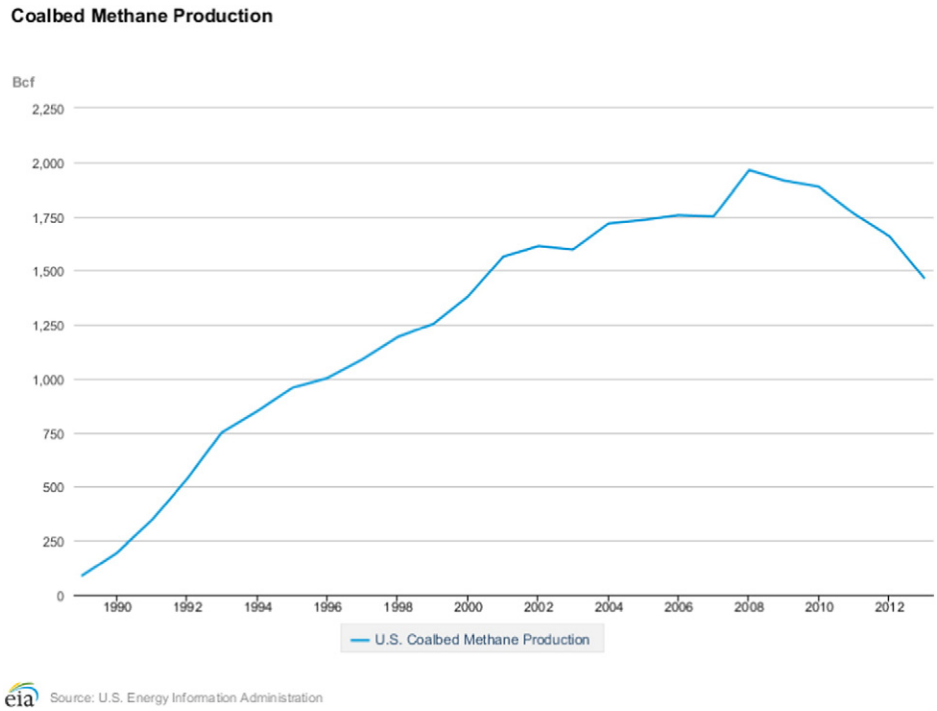

Fig. 1. Annual CBM production in the USA from 1989 to 2013 (EIA, 2014).

flow, diffusion and gas slippage (Cui et al., 2009; Javadpour, 2009). Since pulse-decay assumes Darcy flow as the only flow regime during permeability test, it is critical to at least address the gas slip effect as a correction to differentiate gas permeability from that of liquids. Klinkenberg (Klinkenberg, 1941) initially identified gas slip effect in porous media flow and introduced apparent permeability as the corrected gas permeability. At a molecular level, gas molecules collide with pore walls and tend to slide at the walls instead of losing velocity during gas flow (Swami, 2012). So it is believed that gas slippage can be significant when the pore throat size is comparable to the mean free path of gas molecules at given pressure and temperature (Amyx et al., 1960). The equation to predict apparent permeability component for Klinkenberg effect is described as:

$$k_a = k_\infty\left(1+\frac{b_k}{p}\right) \tag{1}$$

where k_a is the corrected permeability, k_∞ is the intrinsic/Darcy permeability, p is pore pressure at each step of experiments and b_k is the Klinkenberg factor shown as (Ertekin et al., 1986; Randolph et al., 1984)

$$b_k = \frac{16c\mu}{w}\sqrt{\frac{2RT}{\pi M}} \tag{2}$$

where c is a constant typically taken as 0.9, μ is the gas viscosity, M is the fluid molecular weight, w is the width of pore throat, R is the universal gas constant, and T is temperature. And when sorptive gas is used in the permeability measurement, its Klinkenberg factor cannot be directly measured since there is a combination of both slippage and sorption-induced swelling/shrinking effects. Therefore, the value of b should be obtained firstly using helium in order to separate slippage effect and shrinkage effect (Harpalani and Chen, 1997). And the equation used to obtain the slip factor for CO_2 is shown as:

$$b_{CO2} = \frac{\mu_{CO2}}{\mu_{He}}\sqrt{\frac{M_{He}}{M_{CO2}}}b_{He} \tag{3}$$

where μ_{CO2} and μ_{He} are the kinetic viscosity for CO_2 and helium, M_{CO2} and M_{He} are the molecular weights for CO_2 and helium, and b_{CO2} and b_{He} are the Klinkenberg factors for CO_2 and helium, respectively.

Since gas slip flow is happening in tight structure during the measurements, by obtaining apparent permeability data through the pulse-decay method with sorption, Klinkenberg correction is able to back estimate the coal intrinsic permeability (Li et al., 2013) which can be further incorporated into existing stress/strain-based coal permeability models to analysis the effective stress influence on permeability and coal structural changes and extrapolate the uniaxial strain condition in the laboratory scale.

Table 1
Comparison and evaluation of different pulse-decay methods.

Method	Description	Comments
Brace et al. (1968)	Original pulse-decay method	Assumed no compressive gas storage and pure Darcy flow
Hsieh et al. (1981)	Presented a general analytical solution for compressive storage of sample	Without considering the effect of gas adsorption/desorption
Dicker and Smits (1988)	Applied compressive storage effect into pulse-decay measurement	
Kamath et al. (1992)	Pulse-decay to interpret the core's heterogeneity	
Jones (1997)	Simplified the compressive storage factor	
Cui et al. (2009)	Added adsorption component in the compressive factor	Considering both compressive storage and adsorption effect
Wang et al. (2011)	Comprehensive pulse-decay test on Anthracite coals	Simply used the original pulse-decay method
Mckernan et al. (2014)	Used oscillating pore pressure method to get pressure decay	

3. Experimental work

The pulse-decay technique was employed to estimate the permeability of anthracite coal. The advantages of this method is that the permeability can be calculated directly from the linear portion of the solution (Kamath et al., 1992) and it is the only option for very low permeability rocks since it is impossible for maintaining steady-state

flow in ultra-low permeability rocks. With the considerations of gas storage/compressibility and non-Darcy components, this method will be suitable to estimate tight reservoir rock permeability.

3.1. Sample procurement and preparation

Blocks of anthracite coal were obtained from Jeddo coal mine located in Hazleton in Luzerne County, Pennsylvania. The proximate analysis is summarized in Table 2 and yielded a fixed carbon percentage of 78.35%. Cylindrical cores were drilled from the anthracite blocks with one-inch in diameter. Following this, the top and bottom of the drilled core was trimmed to ~2 in. in length and the surfaces were polished to enable proper placement in the triaxial cell. Two well-prepared samples were shown in Fig. 2. After the sample cores were dried, they were then preserved in a dry and clean plastic sample bag in a lab-use alloy box for 3 h before being put into triaxial cell, in order to maintain the integrity of each sample.

3.2. Experimental boundary conditions

To estimate the permeability change under various stress–strain conditions, two boundary conditions were mimicked in our laboratory, that is, constant stress boundary and uniaxial strain boundary conditions. In triaxial cell test, the constant stress condition refers to both the axial and confining stresses were maintained at a constant value throughout the course of experimental duration. The stresses are generated and maintained by computer-controlled syringe pumps. The constant stress boundary condition was relatively easy to achieve. To better replicate in situ condition, the uniaxial strain condition was also implemented in our measurements. Under this condition, the circumferential dimension of the sample and the vertical stress were maintained constants (Palmer and Mansoori, 1998; Shi and Durucan, 2005). Consequently, the horizontal stress was adjusted to maintain the zero net horizontal strain with gas injection or depletion. By comparing the results obtained from both boundary conditions, a quantitative analysis was carried out in this study.

3.3. Experimental setup and procedure

Fig. 3 shows the whole experimental system in our laboratory. The setup includes a Temco triaxial cell core holder, two ISCO syringe pumps, flow rate and pressure monitoring and recording systems. The syringe pumps are capable of maintaining or changing stresses in a controlled manner to the desired stress values. Software panel, a desktop LabVIEW software control panel, is programmed to accurately control the pumps and record the stresses and injection/ejection volumes of fluid. A rubber jacket is used to isolate the sample from the confining fluid. The experimental temperature was kept constant at 296 K (23 °C). The sample was sandwiched between two steel loading platens and then placed inside the core holder. Two comparable fixed volumes, large diameter Swagelok tubing, serve as the upstream and downstream gas reservoirs. The volumes of up-/downstream reservoir are 30,777 mm^3 and 18,526 mm^3, while the sample volume is 26,602 mm^3. Two high-accuracy USB-based Omega pressure transducers were installed to continuously monitor and record pressure–time responses with high sampling rate during the experimental measurements. The pressure-decay pressure curves will be used to estimate the permeability. We conducted the pulse-decay with both helium and CO_2 as the test fluids.

Table 2
Proximate analysis of Pennsylvania anthracite coal sample.

Proximate analysis			
Fixed carbon	Moisture	Ash content	Volatile matter
78.35%	1.59%	10.79%	9.27%

Fig. 2. Photograph of cylindrical Hazelton anthracite core samples.

3.3.1. Helium depletion under constant stress condition

As a non-sorbing gas, helium was firstly chosen to test the coal flow property. The sample was gradually stressed to 1000 psi for the confining stress and 2000 psi for the axial stress. After the mechanical equilibrium was achieved, the entire system was vacuumed by a vacuum pump to remove the residual air in the gas flow system. In order to mimic the in situ gas production procedure, gas depletion was employed. Helium was injected at 950 psi for both upstream and downstream. After the equilibrium was reached, the downstream was reduced to 800 psi, and in this way a pressure difference ("pressure-pulse") between up- and down-stream was created. Then the valves between sample and downstream were opened to discharge the gas through the sample to downstream reservoir. The permeability was estimated based on the pressure–time responses. Following this, the downstream pressure was decreased for next pressure step. Step-wise depletions were carried out with similar interval for designed number of times up to the final equilibrium pressure ~100 psi.

3.3.2. Helium depletion in uniaxial strain/in situ condition

In order to implement the uniaxial strain/in situ condition, the confining stress was passively adjusted to maintain the constant horizontal dimension at each pressure step, meanwhile, the vertical/axial stress was kept constant at 2000 psi. During the experiment, the water was injected into the triaxial cell to create the confining stress. To replicate the in situ condition, the key is to maintain the zero horizontal strain. We continuously monitored the water volume inside the triaxial cell to implement the zero horizontal strain. The change of the water volume inside the cell was equal to the volume change inside the pump because they are a close system. Therefore, we recorded the water volume in the pump and estimated the water volume in the cell. By using this volume change, we can estimate the dimension change of the sample inside the cell. During the experiment, the deformation of rubber jacket was subtracted from the overall volumetric strain change in the cell. A compression test was carried out to obtain a quantitative relationship between rubber jacket deformation and the applied confining stress. A steel rod with the same diameter and length was placed in the cell and then the rubber jacket deformation was continuously recorded with the confining stress from 50 psi to 2500 psi. A linear relationship between the confining stress and rubber jacket thickness deformation is shown in Fig. 4. Taking the rubber deformation into account, we can accurately maintain the constant horizontal dimension by adjusting the confining stress. The constant axial stress was achieved

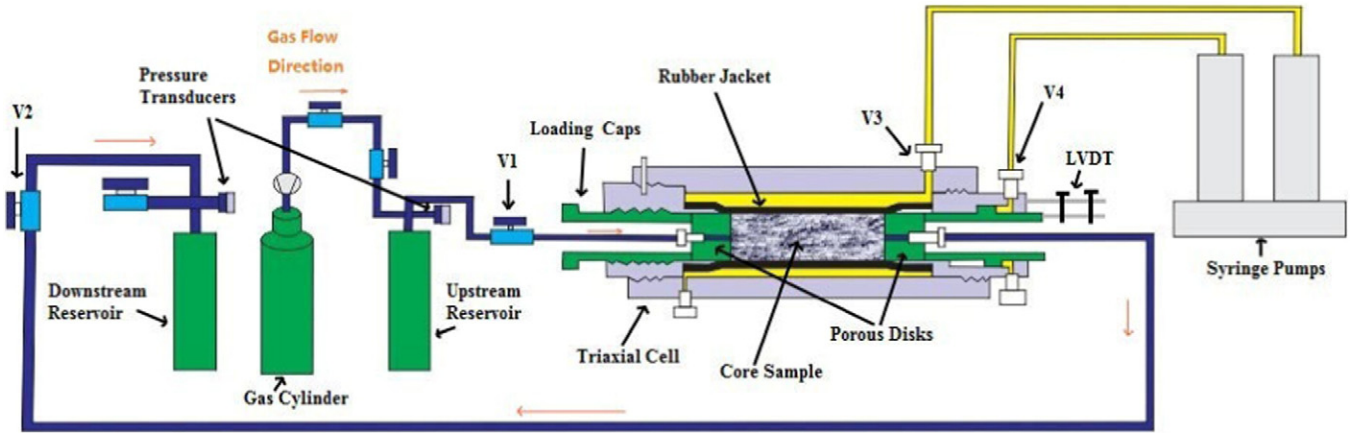

Fig. 3. Picture of the pulse-decay experimental setup for permeability evolution test. V1 is the valve controlling inlet gas flow from upstream, V2 is the valve controlling outlet gas flow to downstream and V3/V4 is the valve controlling the confining/axial stress applied on the sample.

by simply setting the constant pumping pressure in axial direction. Similar to constant stress condition, the sample was depleted from ~950 to ~100 psi with maintaining uniaxial strain condition. The sample was initially stressed to 1070 in confining stress and 2000 psi in vertical stress. During depletion, the permeability at each pressure step was estimated and the corresponding confining stresses were also recorded.

3.3.3. CO_2 depletion permeability measurements

After the helium cycle, CO_2 was used for sorbing gas permeability measurements. In order to make comparison, the external stresses were set the same as the helium depletion, namely, 1000 psi for confining and 2000 psi for axial stresses. And similar depletion steps were applied from ~900 psi to ~100 psi. The permeability was estimated as each pressure step.

After the constant stress boundary condition, we tried to replicate the uniaxial strain condition. Unfortunately, the sample fails during the CO_2 depletion which may be attributed to the "coal weakening" and/or high deviatoric stresses (Harpalani and Mitra, 2009). Thus, we did not report the data for the uniaxial strain CO_2 depletion.

3.4. Pulse-decay permeability estimation

The transient pulse-decay approach provides an effective way to measure the gas permeability of tight rocks. To determine the permeability, the pressure transient equation was introduced by Brace et al. (1968) shown in Eqs. (4) and (5):

$$P_u(t) - P_d(t) = (P_u(t_0) - P_d(t_0))e^{-\alpha t} \tag{4}$$

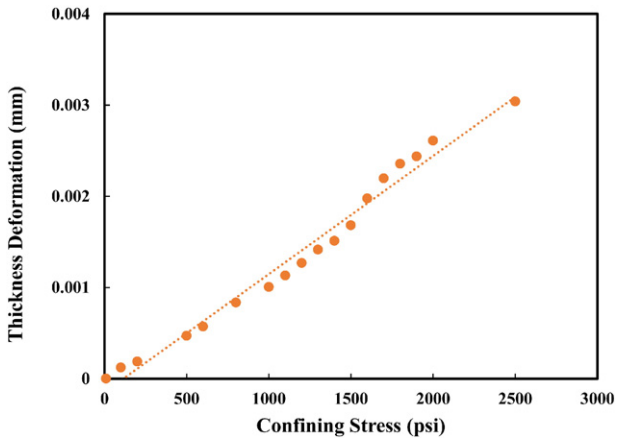

Fig. 4. Rubber jacket deformation evolution with confining stress (linear relationship).

$$\alpha = \left(\frac{k_a A}{\mu c_g L}\right)\left(\frac{1}{V_u} + \frac{1}{V_d}\right) \tag{5}$$

where $P_u(t)$ and $P_d(t)$ are the upstream and downstream pressures at time t, $P_u(t_0)$ and $P_d(t_o)$ are the initial upstream and downstream pressures respectively, α is the slope of the line when plotting the pressure decay $P_u(t) - P_d(t)$ on semi-log paper against time, A is the cross-sectional area of the sample, L is the length of sample, c_g is gas compressibility, and V_u and V_d are the upstream and downstream reservoir volumes respectively. After pressure data are collected from experiments, the only unknown will be sample permeability k which can be estimated.

This classic method was still one of the most popular methods to estimate the low-permeability rocks, but it is questionable whether this method can be directly applied to compressible testing fluids. Brace et al. (1968) assumed Darcy flow only during the measurement and no compressive storage in the rock sample for the testing fluids. It was a good assumption if the testing fluid is water or liquids that can be treated as incompressible fluid in the testing pressure range. However, the gas is known to be highly compressible that the storage volume should be corrected to get the real gas transport properties. To compute both permeability and specific storage of the test sample experimentally, Hsieh et al. (1981) derived more restrictive analytical solutions of the differential equation describing the decay curves from the permeability measurement with compressive storage effect. The general solution of the differential equation for dimensionless pressure difference and dimensionless time was improved and shown as Dicker and Smits (1988):

$$\Delta p_D = 2\sum_{n=1}^{\infty} \frac{a\left(b^2+\theta_n^2\right) - (-)b\sqrt{\left(a^2+\theta_n^2\right)\left(b^2+\theta_n^2\right)}}{\theta_n^2\left(\theta_n^2 + a + a^2 + b + b^2\right) + ab(a+b+ab)} \times e^{\left(-\theta_n^2 t_d\right)} \tag{6}$$

where, a and b are the ratios of sample's storage capacity to that of upstream reservoir and downstream reservoir, and θ_n is the nth root of the following equation:

$$tan\theta = \frac{(a+b)\theta}{\theta^2 - ab} \tag{7}$$

where $a = \frac{V_p}{V_u}$, $b = \frac{V_p}{V_d}$ and V_p are the pore volumes of rock sample.

To simplify the above method, Jones (1997) introduced a factor f as follows:

$$f = \frac{\theta^2}{a+b} \tag{8}$$

and the original pulse-decay equation turns into:

$$\alpha = \left(\frac{f k_a A}{\mu c_g L}\right)\left(\frac{1}{V_u}+\frac{1}{V_d}\right). \quad (9)$$

Then the measured sample permeability becomes:

$$k_a = \frac{\alpha \mu c_g L}{fA\left(\frac{1}{V_u}+\frac{1}{V_d}\right)}. \quad (10)$$

Another feature of the organic-bearing rocks is adsorption. The Dicker & Smits's method can correct the compressive storage, but it could not handle the loss of adsorbed gas during the gas injection because the adsorbed gas is no longer in gaseous phase. In order to extend the pulse-decay technique for sorptive and tight material, Cui et al. (2009) presented a new approach to estimate permeability with both pore compressive storage effect and sorption effect for organic-bearing rocks. Corresponding to the effective porosity of core sample, an effective adsorption porosity term is introduced to account for the contribution off gas molecule adsorption. Langmuir model was used to quantify the gas adsorption volume as a function of pressure (Langmuir, 1918) and mathematically described as follows:

$$V_a = \frac{V_L p}{p_L + p} \quad (11)$$

where, V_a is the gas adsorbed volume, V_L is the Langmuir volume and p_L is the Langmuir pressure. So the sample storage capacity ratio in Cui et al.'s approach becomes:

$$a = \frac{V_p\left(1+\frac{\phi_a}{\phi}\right)}{V_u} \quad (12)$$

$$b = \frac{V_p\left(1+\frac{\phi_a}{\phi}\right)}{V_d} \quad (13)$$

where, $\phi_a = \frac{\rho_s(1-\phi)p_L V_a}{\rho V_{std} C_g (p_L+p)^2}$, ϕ is the matrix porosity of rock sample, ρ and ρ_s are the molar density of gas and the skeleton density of porous sample respectively, and V_{std} is the molar volume of gas at standard pressure and temperature (i.e. 273.15 K and 101,325 Pa). In this study, we compared the estimated permeabilities by different aforementioned approaches including the classic Brace approach, Dicker & Smits method and Cui et al. approach, and recommendations were made for the tight anthracites.

4. Results and discussion

4.1. Pulse-decay pressure curve comparison between helium and CO_2

Fig. 5 shows the helium and CO_2 pulse-decay pressure response curves measured at each gas pressure step during constant stress conditions. Due to the fact that equilibrium time is extremely long (may last for more than 1 week at 100 psi gas pressure) at low pressure, we only took partial pressure-decay curve to estimate the permeability. This is an advantage feature of the transient method. From Fig. 5, we found that the time required to approach the equilibrium decreases as increase of injection pressure for both helium and CO_2. Considering helium as a non-sorbing gas, only effective stress effect influences the permeability evolution, and the permeability are expected to increase with elevated pore pressure at which the effective stress reduced correspondingly.

For CO_2 gas, beside the effective stress effects, the sorption process, happened on the internal surface of coal matrix, influences the structure of coal matrix and thus the gas deliverability. Driven by multiple mechanisms, the permeability of CO_2 is expected to follow different variation trend compared to helium which will be directly captured and visualized from the pressure curves. From Fig. 5, the CO_2 gas pressure equilibrium time, as we can observe, is generally more than that for helium, which physically indicates CO_2 transport slower than helium under similar conditions. And the pressure decay rate is lower between 300 and 500 psi than other pressures, which indicates a lower permeability in this pressure range.

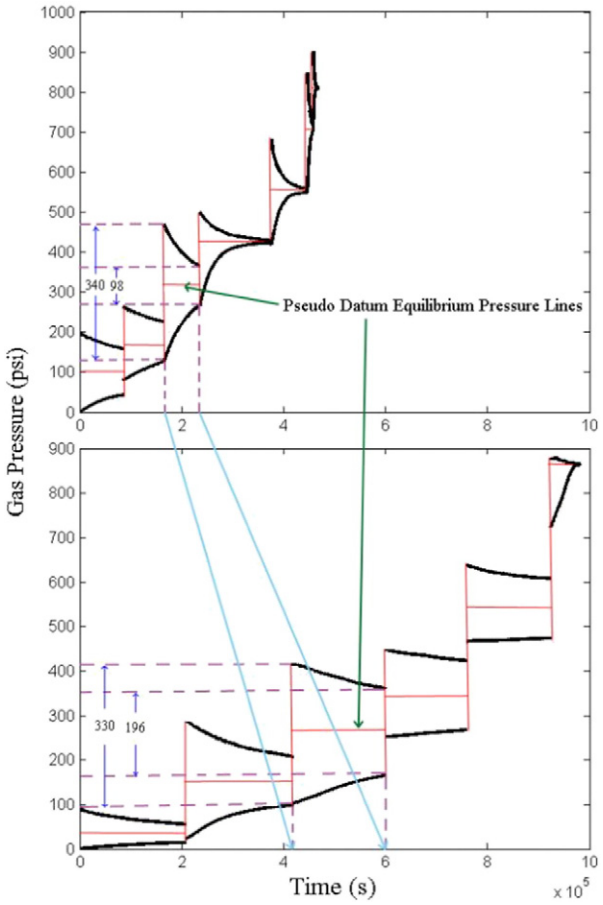

Fig. 5. Comparison of pulse-decay pressure responses for helium and CO_2 injections. The pressure equilibrium time for helium is at least 30 h less than that of CO_2 at each pressure step. At high pressure helium pressure can get equilibrium in a relatively short time while the CO_2 pressure yet have a longer equilibrium time.

If we make a careful comparison with helium and CO_2 pressure decay curves, a few notable findings can be observed qualitatively. According to Fig. 5, the overall time for helium permeability measurement is just as half as the time for CO_2, and even that a few helium curves already get equilibrium while most the CO_2 still on its half way at most pressure steps. For example, when the pseudo equilibrium pressure is about 300 psi (upstream pressure about 400 plus and downstream pressure about 100 plus for both gases), the helium pressure difference between upstream and downstream reservoir change from 340 to 98 psi within less than 1×10^5 s while it took almost 2×10^5 s for the CO_2 pressure difference to only vary from 330 to 196 psi. With this comparison, we can conclude that it requires much more time for the equilibrium for CO_2 than for helium to pass through the rock sample at same condition, which indicates the helium gas permeability is higher than the CO_2 gas permeability. This also indicates the coal permeability is a gas type dependent property. For non-sorbing gas, the total free gas keeps constant in the whole system. However, for anthracite coal and other sorptive reservoir rocks, the gas ad-/desorption process can either store in or produce gas from the matrix, dominating

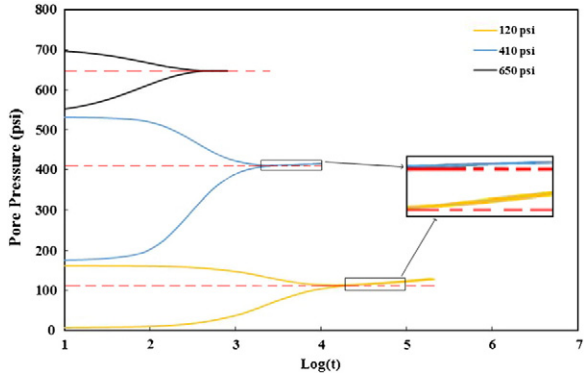

Fig. 6. Carbon dioxide pulse-decay pressure curves at three different pore pressures under constant stress condition in gas depletion process.

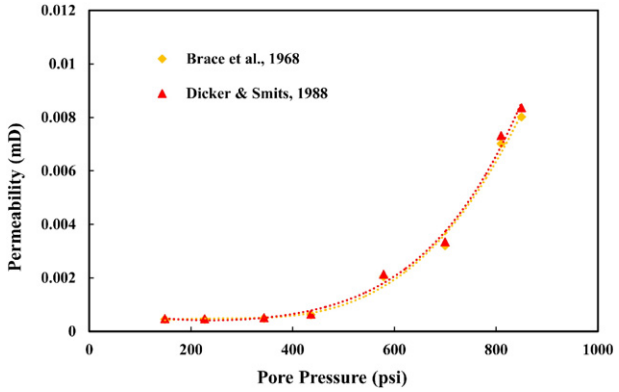

Fig. 8. Helium permeability profiles under uniaxial strain condition, obtained by Brace's and Dicker & Smits's methods respectively.

the flux in/out the matrix. In Fig. 5, we can observe several obvious asymmetries for CO_2 depletion. For example when the pseudo equilibrium pressure at 550 psi, the upstream pressure drops in a higher speed from 640 to 600 psi while the downstream pressure hardly has any increment larger than a few psi. This indicates that the absolute free gas quantify decrease as time elapse. This lost gas quantity should be considered during the permeability measurement.

In order to qualitatively analyze the sorption effect on the pressure decay cures, we repeat three pressure decays for the same coal sample under the same experimental condition where we allowed fully equilibrium as shown in Fig. 6. The sample was depleted from ~700 psi. The dot lines represent the pseudo equilibrium pressure at each pressure step. One interesting observation is that the equilibrium pressure slightly increases with time elapse at 410 and 120 psi, which indicates there is extra gas mass influx to the free gas phase. This may be attributed to the slow gas desorption with gas depletion. Because desorption is a slower process than pressure-driven flow. Conceptually, the equilibrium takes two coherent processes: one is the pressure drive equilibrium where the pressure equilibrium between up- and down volume happens relatively fast; the other is desorption-driven flow which happens relatively slow. This desorption-driven flow makes the tails of pressure equilibrium slightly upwards instead of maintaining stationary at low pressures. And this effect is hardly seen at high pressure because of the nature of the sorption behavior that sorption reach the plateau at high pressures for coals (Busch et al., 2004; Harpalani et al., 2006).

If we look into different scale of this phenomenon, we may see that the ad-/de-sorption effect has the real influence on the permeability evolution during reservoir pressure change. For unconventional reservoirs, the adsorption effect provides a large gas storage capacity while the desorption process leads to a significant increment on the total non-Darcy flux, and thus may control late-time production reservoir behavior, if desorption/diffusion is the rate-limiting step (Cui et al., 2009; Yi et al., 2008). Besides, the shrinkage of matrix due to desorption effect also results in the rock matrix deformation and, consequentially, permeability change (Kumar et al., 2014, 2012; Liu and Harpalani, 2013a; Wang et al., 2012).

4.2. Helium permeability results under constant and uniaxial strain condition

As Section 3.4 mentioned, the compressive storage could cause the error in the permeability estimation. We quantitatively analyzed how compressive storage influences the permeability estimation here. Since helium is a non-sorbing gas, helium permeability was estimated under constant stress condition obtained by Brace's method (without compressive storage correction) and Dicker & Smits's method (with compressive storage correction). In order to apply Dicker & Smits's method, the initial porosity is required and was assumed to be 8% (Gan et al., 1972; Rodrigues and Lemos De Sousa, 2002). For both methods, the permeabilities were estimated and plotted in Fig. 7. The permeability decreases from ~0.01 to ~0.0002 md with pore pressure decreasing from 900 to 100 psi. Although Dicker & Smits's method includes the compressive storage effect, there is almost no difference between the two permeability profiles. This is not surprising since the anthracite coal has really low porosity. This has been confirmed for the uniaxial strain condition with the results shown in Fig. 8. The permeabilities estimated by both methods were very similar.

In order to test how the contribution of pore volume compressive storage varies with pore volume, we calculated the permeability difference in percentage between Brace's method and Dicker & Smits' method, within a porosity range between 5% and 30%. Fig. 9 shows the

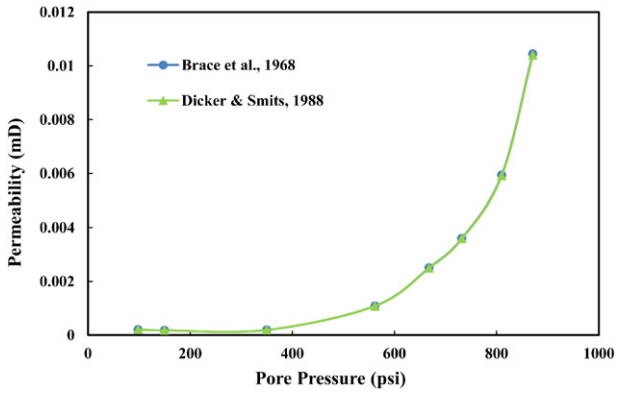

Fig. 7. Helium permeability profiles under constant stress condition, obtained by Brace's and Dicker & Smits's methods respectively.

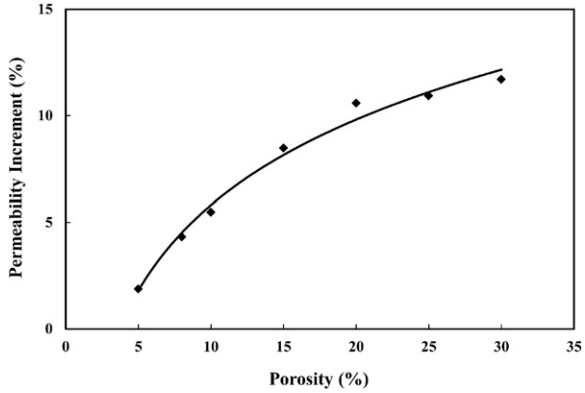

Fig. 9. Permeability increments of Dicker & Smits's method comparing to Brace's method at constant pressure at 350 psi.

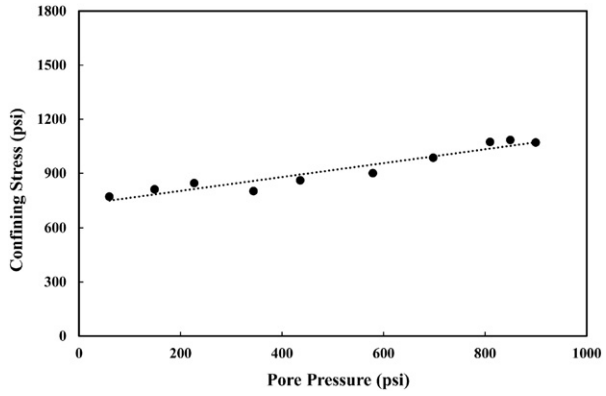

Fig. 10. Horizontal stress variation for helium depletion under uniaxial strain condition.

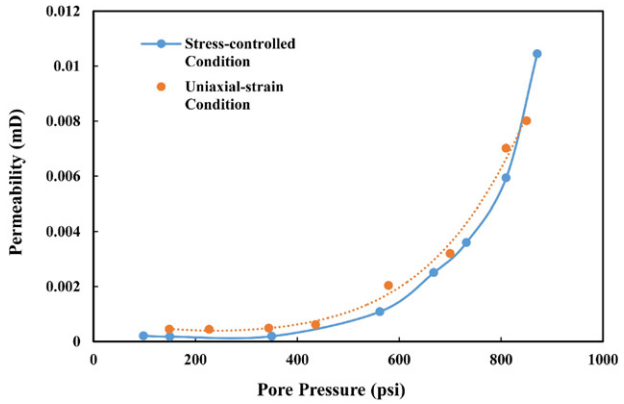

Fig. 12. Permeability evolution with helium depletion under both constant stress and uniaxial strain condition using Dicker & Smits's method.

permeability difference between Dicker & Smits's method and the original Brace's method. The difference between the two methods increases with the increase of sample porosity. With the porosity below 10%, Dicker & Smits's estimated values are at most 5% larger than Brace's method. When the sample porosity increases to 30%, this difference can become up to 12%. Note that in this study the sample volume is not so different with up-/downstream reservoir volume, and the pore volume takes up only 6% of upstream volume and 11% of downstream volume. Consequently, we may safely assume that at a relative low pressure for non-sorbing gas, the pore compressive storage effect, in our case when the sample volume is quite small compared to up-/downstream volume, is insignificant and thus there is no significant difference between Brace's method and Dicker & Smits's method. Either method can be used predict the permeability at both constant stress condition and uniaxial strain condition. For other type of ultra-tight rocks, the compressive storage may not be significant due to the low porosity nature. Therefore, it would be a good assumption that for shale and tight reservoirs, Brace's method can be safely applied for the non-sorbing gas permeability estimation at relatively low pressures.

Now we compare the permeability results obtained by Brace's method under two boundary conditions. Differed from stress-controlled condition, horizontal stress decreased from 1070 to 770 psi for pore pressure depletion from 850 to 150 psi, as shown in Fig. 10. The effective horizontal stress for both boundary conditions were calculated and shown in Fig. 11. With depletion, the increase of effective horizontal stress for uniaxial strain condition is slower than for constant stress condition. The reason is simply because horizontal stress under uniaxial strain condition kept decreasing to maintain the zero horizontal strain resulting in a relatively slow effective horizontal stress increase. This phenomenon has been observed for low rank coals in our previous studies (Liu and Harpalani, 2014c; Harpalani and Mitra, 2009). As expected,

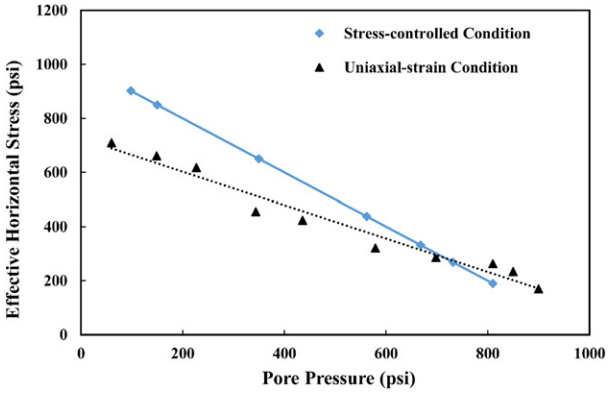

Fig. 11. Change in effective horizontal stress with helium depletion under two different stress–strain conditions: uniaxial strain and constant stress.

the permeability under uniaxial strain conditions was found to be higher than the constant stress condition as shown in Fig. 12 and Table 3. These results well correlate to the effective stress variations as Fig. 11. With increase of effective stress, the permeability decreases with depletion.

4.3. CO_2 gas permeability results with stress-controlled condition

In order to test influence of different pulse-decay calculation methods for sorbing gas, CO_2 depletion was conducted under constant stress condition. Based on the pressure response curves obtained during the experiment, comparisons were made between the three pulse-decay calculation methods, original pulse-decay (Brace et al., 1968), modified method with pore compressive storage effect (Dicker and Smits, 1988) and modified method with sorption effect (Cui et al., 2009). The results were shown in Fig. 13. The permeability was calculated using three methods. In order to take the sorption into consideration in Cui et al.'s method, the sorption data were measured in our lab, including Langmuir pressure ($p_L = 200$ psi), Langmuir volume ($V_L = 24$ ml/g), sample length ($L = 52.5$ mm), temperature ($T = 295.15$ K). Gas properties and other pressure–temperature dependent parameters were calculated by following the ASTM standard methods.

In Fig. 13, the calculated permeabilities using three different pulse-decay methods behave somewhat similar. The permeability initially declines sharply with pressure-depletion from 850 to 400 psi and then start to respond. It is well known that the gas permeability in coal was simultaneously controlled by the effective stress and microstructural change due to sorption known as matrix shrinkage (Cui and Bustin, 2005; Palmer and Mansoori, 1998; Shi and Durucan, 2005). The initial permeability decrease was attributed to the effective increase as shown in the figure. Although the desorption-induced shrinkage happens in these high pressures, but the dominate effect is the increase of effective stress tending to narrow the gas flow channels. When the pore pressure keeps decreasing, a significant portion of CO_2 will desorb from the matrix and this sorption induced permeability increase will dominate the flow behaviors in the low pressures. Because of matrix shrinkage effect, permeability tends to increase though the effective stress increases. This CO_2 permeability behavior in pulse-decay test

Table 3
Experimental data of helium permeability (mD) under stress-controlled and uniaxial-strain conditions.

	Pore pressure (psi)					
Pulse-decay method	150	230	350	440	580	700
Stress-controlled	0.000449	0.000442	0.000486	0.000614	0.00204	0.00320
Uniaxial-strain	0.000469	0.000461	0.000507	0.000640	0.00213	0.00334

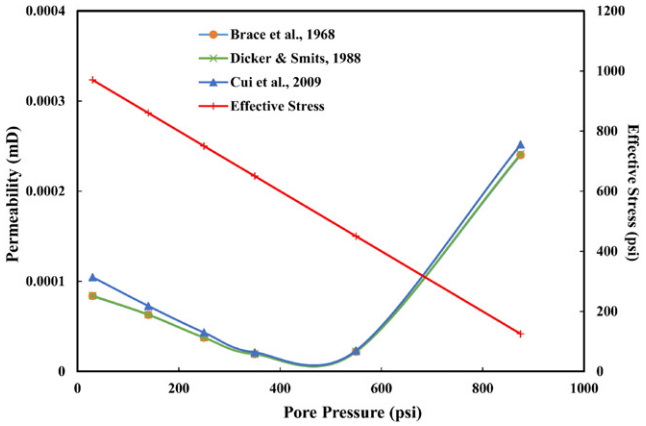

Fig. 13. Comparison between three different pulse-decay methods with effective stress.

matches previous laboratory measurements on tight coal samples done by several researchers (Izadi and Elsworth, 2013; Li et al., 2013; Wang et al., 2011). However, the permeability did not recover to or exceed its original values for anthracite, which is different from some of the low-rank coals (Liu and Harpalani, 2013b; Mitra et al., 2012). This might be due to the tight structure of anthracite and the sorption induced matrix shrinkage is comparatively less than bituminous coals.

Comparing the permeability data from original pulse-decay method, the result from Dicker & Smits's method still shows almost no difference with Brace's method, indicating the pore compressive effect at low pressure is also less significant with CO_2 gas, as we can see from the values in Table 4. On the other hand, at low pressure less than 100 psi, there is an obvious enhancement in Cui et al.'s model. By considering the sorption effect, the Cui et al.'s method estimates higher permeability than the other two methods, especially at low pressure. For example, the estimated permeability Cui et al.'s approach is 28% higher than the other two at 30 psi pore pressure. The reason why the estimated permeability deviation is elevated is that the sorption effect becomes more significant at low pressure. And clearly this sorption process during gas depletion has a positive influence on the permeability. The contribution of sorption to overall multi-mechanistic flow is thus important and the pulse-decay method with sorption correction significantly benefits experimental characterization of tight rock permeability.

In order to test whether the found permeability results were comparable with the reported results for the similar coal or not, a quantitative comparison was conducted between the experimental data from Wang et al. (2011) and this study (Fig. 14). In Wang et al.'s work, the coal sample was collected from the Northumberland Basin, Mount Carmel in Pennsylvania. Similar experimental setup was used for pulse-decay and a constant confining/axial stress of 6 MPa (870) was applied. The method they followed is Brace's method. Compared to our data with Brace's method, the permeability values from Wang et al.'s work is very close to our results, and the permeability evolutions share the same trend as "check-shape". Overall their values are higher than ours. This may be attributed to the lower external stresses they applied, since less external stress generally resulted in less effective stress and higher permeability. Although other factors, such as mineral contents, adsorption capacity, physical properties, and cleat spacing, may contribute to the permeability difference.

4.4. Intrinsic permeability prediction

Generally speaking, rock's intrinsic permeability obtained by Klinkenberg correction can be lower than the apparent permeability, because slip effect is such a phenomenon showing that gas permeability potentially is higher than pure liquid permeability at the same condition. The influence of Klinkenberg effect on low permeability reservoirs will increase with the reduction of gas pressure (Wang et al., 2014). To apply the Klinkenberg correction, the average width of pore throat in anthracite coal is assumed to be 0.001 μm in this study (Halliburton Company, 2007). The apparent permeability data obtained by the above experiments were reduced by Klinkenberg correction to the intrinsic permeability. We took Cui et al. method's result only since the other two methods follow the same behavior and the result was shown in Fig. 15. The intrinsic permeability starts to deviate from the measured apparent permeability from 180 psi. There is a 20% reduction of permeability value comparing to the apparent permeability at 30 psi. On the contrary, the intrinsic permeability is almost the same with the apparent permeability above 180 psi. This phenomenon consists with the most recently findings for the tight shales that the slip flow play increasingly important role at low pressures and is minimal at high pressures (Civan et al., 2011; Javadpour, 2009; Javadpour et al., 2007). Therefore, based on the obtained results, we may see the importance of non-Darcy flow on tight rock permeability measurement and analysis.

5. Conclusion

A series of experimental studies and theoretical analyses on permeability of Hazelton anthracite core sample under different stressed controlled conditions has been presented. The results show that the permeability evolution of studied coal is pressure-boundary dependent and it is simultaneously controlled by the effective stress profile and the sorption process which tends to alter the microstructure of coal. Three different pulse-decay calculation methods for conventional and unconventional gas permeability are utilized and compared. Based on the work completed, the following conclusions are made and summarized:

1. Under uniaxial strain condition, the applied horizontal stress linearly decreased with gas pressure depletion, which consists with traditional oil/gas reservoirs. Because of the horizontal stress loss, the permeability under constant stress condition with helium depletion was found to be less than the results under uniaxial strain condition.
2. The sorption induced matrix shrinkage plays important role on the permeability enhancement at low pressure for the anthracite coal. But it is not strong enough to compensate the stress effect as the bituminous coal did.
3. For the pulse-decay method, the contribution of ad-/desorption can be clearly observed from the pressure respond curves. And this effect is stronger at low pressure than high pressures.
4. Comparing Brace's method and Dicker & Smits's method, Dicker & Smits's method incorporates the pore compressive storage effect

Table 4
Experimental data of CO2 permeability (mD) by using different pulse-decay approaches.

	Pore pressure (psi)					
Pulse-decay method	30	140	250	350	550	875
Brace et al. (1968)	8.36E−05	6.28E−05	3.75E−05	1.91E−05	2.18E−05	2.4E−04
Dicker and Smits (1988)	8.40E−05	6.31E−05	3.76E−05	1.92E−05	2.19E−05	2.4E−04
Cui et al. (2009)	1.05E−04	7.26E−05	4.31E−05	2.12E−05	2.33E−05	2.5E−04

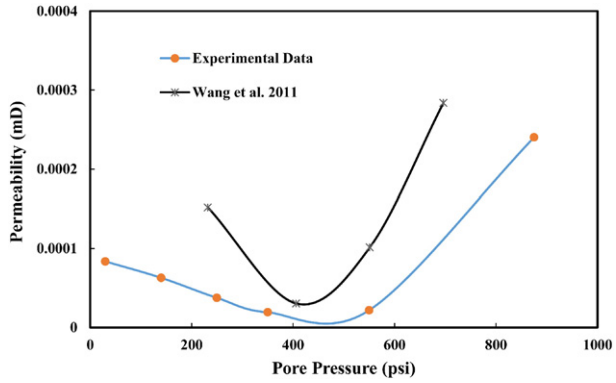

Fig. 14. Experimental result comparison with anthracite CO_2 permeability data by Wang et al. (2011).

only and it may have more influence on gas permeability at pressure higher than 1000 psi. On the other hand, these two methods can be identical and both valid at relatively low pressure. For simplicity, Brace's method gives reliable data at the range of investigated pressures for tight and ultra-tight rocks.

5. Cui et al.'s method gives an obvious enhancement for the contribution of sorption effect in permeability calculation, providing a good direction of how the gas sorption effect can help to predict apparent permeability.
6. Based on the data observation, at extremely low permeability the Klinkenberg effect becomes significant, and gas slippage is considered to be an important effect when predicting unconventional reservoir gas permeability due to multiple flow mechanism. The characterization of gas slip flow, along with sorption and other non-Darcy flow components, plays an important role in both production analysis and laboratory measurement. It is worthwhile to pay more attention on how to measure and calculate the apparent permeability in a laboratory scale with so many non-Darcy components in future study.

Acknowledgements

This work is supported in part by NSF CBET — Fluid Dynamic Program (CBET — 1438398) and by Open Research Project through State Key Laboratory of Coal Resources and Safe Mining from China University of Mining and Technology at Beijing (SKLCRSM13KFA01). The authors would also like to acknowledge James R. Pagnotti and Eric T. Bella from Pagnotti Enterprises, Inc. for the sample collection and preparation.

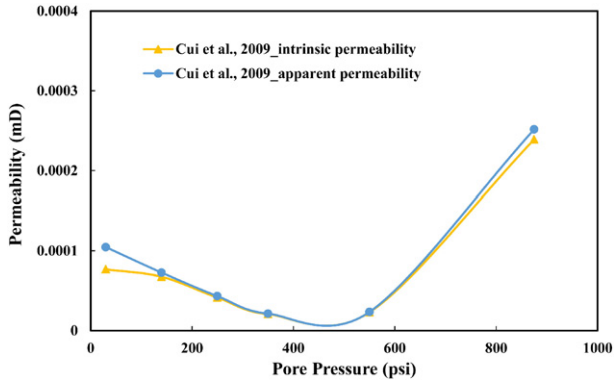

Fig. 15. Comparison between intrinsic permeability and apparent permeability obtained by Cui et al.'s methods.

References

Amyx, J.W., Bass, D.M.J., Whiting, R.L., 1960. Petroleum Reservoir Engineering.
Brace, W.F., Walsh, J.B., Frangos, W.T., 1968. Permeability of granite under high pressure. J. Geophys. Res. 73.
Breckels, I.M., Eekelen, H.A.M., 1982. Relationship between horizontal stress and depth in sedimentary basins. J. Pet. Technol. 34, 2191–2199. http://dx.doi.org/10.2118/10336-PA.
Busch, A., Gensterblum, Y., Krooss, B.M., Littke, R., 2004. Methane and carbon dioxide adsorption–diffusion experiments on coal: upscaling and modeling. Int. J. Coal Geol. 60, 151–168. http://dx.doi.org/10.1016/j.coal.2004.05.002.
Civan, F., Rai, C., Sondergeld, C., 2011. Shale-gas permeability and diffusivity inferred by improved formulation of relevant retention and transport mechanisms. Transp. Porous Media 86, 925–944. http://dx.doi.org/10.1007/s11242-010-9665-x.
Coal Age, 2014. DEC 2014.
Cui, X., Bustin, R.M., 2005. Volumetric strain associated with methane desorption and its impact on coalbed gas production from deep coal seams. Am. Assoc. Pet. Geol. Bull. 89, 1181–1202. http://dx.doi.org/10.1306/05110504114.
Cui, X., Bustin, A.M.M., Bustin, R.M., 2009. Measurements of gas permeability and diffusivity of tight reservoir rocks: different approaches and their applications. Geofluids 9, 208–223. http://dx.doi.org/10.1111/j.1468-8123.2009.00244.x.
Dicker, A.I., Smits, R.M., 1988. A practical approach for determining permeability from laboratory pressure-pulse decay measurements, SPE International. Meeting on Petroleum Engineering, Tianjin, China, 1–4 Nov, 1998 (Tianjin, China.).
EIA, 2014. U.S. Coalbed Methane Production (Billion Cubic Feet) [WWW Document] http://www.eia.gov/dnav/ng/hist/rngr52nus_1a.htm (accessed 8.4.15).
Ertekin, T., King, G., Schwerer, F., 1986. Dynamic gas slippage: a unique dual-mechanism approach to the flow of gas in tight formations. SPE Form. Eval. http://dx.doi.org/10.2118/12045-PA.
Gan, H., Nandi, S.P., Walker, P.L., 1972. Nature of the porosity in American coals. Fuel 51, 272–277. http://dx.doi.org/10.1016/0016-2361(72)90003-8.
Geertsma, J., 1966. Problems of rock mechanics in petroleum production engineering. 1st ISRM Congr 3 pp. 585–594.
Gensterblum, Y., Ghanizadeh, A., Krooss, B.M., 2014. Gas permeability measurements on Australian subbituminous coals: fluid dynamic and poroelastic aspects. J. Nat. Gas Sci. Eng. 19, 202–214. http://dx.doi.org/10.1016/j.jngse.2014.04.016.
Halliburton Company, 2007. Chapter 04 — reservoir analysis. Coalbed Methane Principles Practpp. 191–282.
Harpalani, S., Chen, G., 1997. Influence of gas production induced volumetric strain on permeability of coal. Geotech. Geol. Eng. 15, 303–325. http://dx.doi.org/10.1007/BF00880711.
Harpalani, S., Mitra, A., 2009. Impact of CO2 injection on flow behavior of coalbed methane reservoirs. Transp. Porous Media 82, 141–156. http://dx.doi.org/10.1007/s11242-009-9475-1.
Harpalani, S., Prusty, B., Dutta, P., 2006. Methane/CO2 sorption modeling for coalbed methane production and CO2 sequestration. Energy Fuel 20, 1591–1599.
Hartman, R., 2008. Recent Advances in the Analytical Methods Used for Shale Gas Reservoir Gas-in-place Assessment. AAPG Annual Convention, San Antonio, Texas (20–23 Apr, 2008).
Heller, R., Vermylen, J., Zoback, M., 2014. Experimental investigation of matrix permeability of gas shales. Am. Assoc. Pet. Geol. Bull. 98, 975–995. http://dx.doi.org/10.1306/09231313023.
Hildenbrand, A., Krooss, B.M., Busch, A., Gaschnitz, R., 2006. Evolution of methane sorption capacity of coal seams as a function of burial history — a case study from the Campine Basin, NE Belgium. Int. J. Coal Geol. 66, 179–203. http://dx.doi.org/10.1016/j.coal.2005.07.006.
Hsieh, P.A., Tracy, J.V., Neuzil, C.E., Bredehoeft, J.D., Silliman, S.E., 1981. A transient laboratory method for determining the hydraulic properties of "tight" rocks—I. Theory. Int. J. Rock Mech. Min. Sci. Geomech. Abstr. 18, 245–252. http://dx.doi.org/10.1016/0148-9062(81)90979-7.
Izadi, G., Elsworth, D., 2013. The effects of thermal stress and fluid pressure on induced seismicity during stimulation to production within fractured reservoirs. Terra Nova 25, 374–380. http://dx.doi.org/10.1111/ter.12046.
Izadi, G., Wang, S., Elsworth, D., Liu, J., Wu, Y., Pone, D., 2011. Permeability evolution of fluid-infiltrated coal containing discrete fractures. Int. J. Coal Geol. 85, 202–211. http://dx.doi.org/10.1016/j.coal.2010.10.006.
Javadpour, F., 2009. Nanopores and apparent permeability of gas flow in mudrocks (shales and siltstone). J. Can. Pet. Technol. 48, 1–6.
Javadpour, F., Fisher, D., Unsworth, M., 2007. Nanoscale gas flow in shale gas sediments. J. Can. Pet. Technol. 46. http://dx.doi.org/10.2118/07-10-06.
Jones, S., 1997. A technique for faster pulse-decay permeability measurements in tight rocks. SPE Form. Eval. 25–28.
Kamath, J., Boyer, R., Nakagawa, F., 1992. Characterization of core-scale heterogeneities using laboratory pressure transients. SPE Form. Eval. 219–227.
Klinkenberg, L.J., 1941. The permeability of porous media to liquids and gases. Drill. Prod. Pract. 57–73. http://dx.doi.org/10.5510/OGP20120200114.
Kumar, H., Elsworth, D., Liu, J., Pone, D., Mathews, J.P., 2012. Optimizing enhanced coalbed methane recovery for unhindered production and CO2 injectivity. Int. J. Greenhouse Gas Control 11, 86–97. http://dx.doi.org/10.1016/j.ijggc.2012.07.028.
Kumar, H., Elsworth, D., Mathews, J.P., Liu, J., Pone, D., 2014. Effect of CO2 injection on heterogeneously permeable coalbed reservoirs. Fuel 135, 509–521. http://dx.doi.org/10.1016/j.fuel.2014.07.002.

Langmuir, I., 1918. The adsorption of gases on plane surfaces of glass, mica and platinum. J. Am. Chem. Soc. 345.
Li, J., Liu, D., Yao, Y., Cai, Y., Chen, Y., 2013. Evaluation and modeling of gas permeability changes in anthracite coals. Fuel 111, 606–612. http://dx.doi.org/10.1016/j.fuel.2013.03.063.
Liu, S., Harpalani, S., 2013a. A new theoretical approach to model sorption-induced coal shrinkage or swelling. Am. Assoc. Pet. Geol. Bull. 97, 1033–1049. http://dx.doi.org/10.1306/12181212061.
Liu, S., Harpalani, S., 2013b. Permeability prediction of coalbed methane reservoirs during primary depletion. Int. J. Coal Geol. 113, 1–10. http://dx.doi.org/10.1016/j.coal.2013.03.010.
Liu, S., Harpalani, S., 2014a. Compressibility of sorptive porous media: part I — background and theory. Am. Assoc. Pet. Geol. Bull. 98, 1761–1772.
Liu, S., Harpalani, S., 2014b. Compressibility of sorptive porous media: part II — experimental study on coal. Am. Assoc. Pet. Geol. Bull. 98, 1773–1788.
Liu, S., Harpalani, S., 2014c. Evaluation of in situ stress changes with gas depletion of coalbed methane reservoirs. J. Geophys. Res. Solid Earth 119, 6263–6276. http://dx.doi.org/10.1002/2014JB011228.Received.
Lorenz, J.C., Teufel, L.W., Warpinski, N.R., 1991. Regional fractures: I. A mechanism for the formation of regional fractures at depth in flat-lying reservoirs. AAPG Bull. 75, 1714–1737.
Luffel, D., Hopkins Jr., C., P.S., 1993. Matrix Permeability Measurement of Gas Productive Shales. SPE Annual Technical Conference and Exhibition, Houston, Texas (2–6 Oct, 1993).
Malkovsky, V.I., Zharikov, A.V., Shmonov, V.M., 2009. New methods for measuring the permeability of rock samples for a single-phase fluid. Izv. Phys. Solid Earth 45, 89–100. http://dx.doi.org/10.1134/S1069351309020013.
Markowski, a.k., 2014. Pennsylvania Coalbed Methane Update 80353.
Markowski, A., Resources, N., Virginia, W., 2014. Coalbed Methane in Pennsylvania.
Mazumder, S., Wolf, K., 2008. Differential swelling and permeability change of coal in response to CO 2 injection for ECBM. Int. J. Coal Geol. 74 (2), 123–138.
Mckernan, R.E., Rutter, E.H., Mecklenburgh, J., Taylor, K.G., 2014. Influence of effective pressure on mudstone matrix permeability: implications for shale gas production. SPE/EAGE European Unconventional Conference and Exhibition. Society of Petroleum Engineers, Vienna, Austria, p. 13 http://dx.doi.org/10.2118/167762-MS (25–27 Feb, 2014).
Mitra, A., Harpalani, S., Liu, S., 2012. Laboratory measurement and modeling of coal permeability with continued methane production: part 1 — laboratory results. Fuel 94, 110–116. http://dx.doi.org/10.1016/j.fuel.2011.10.052.
Palmer, I., Mansoori, J., 1998. How permeability depends on stress and pore pressure in coalbeds: a new model. SPE Reserv. Eval. Eng. SPE 52607, 539–544.
Pan, Z., Connell, L.D., 2007. A theoretical model for gas adsorption-induced coal swelling. Int. J. Coal Geol. 69, 243–252. http://dx.doi.org/10.1016/j.coal.2006.04.006.
Pillalamarry, M., Harpalani, S., Liu, S., 2011. Gas diffusion behavior of coal and its impact on production from coalbed methane reservoirs. Int. J. Coal Geol. 86, 342–348. http://dx.doi.org/10.1016/j.coal.2011.03.007.
Randolph, P.L., Soeder, D.J., Chowdiah, P., 1984. Porosity and Permeability of Tight Sands. SPE Unconventional Gas Recovery Symposium, 13-15 May, Pittsburgh, Pennsylvania.
Rodrigues, C.F., Lemos De Sousa, M.J., 2002. The measurement of coal porosity with different gases. Int. J. Coal Geol. 48, 245–251. http://dx.doi.org/10.1016/S0166-5162(01)00061-1.
Shi, J.Q., Durucan, S., 2004. Drawdown induced changes in permeability of coalbeds: a new interpretation of the reservoir response to primary recovery. transp. Porous. Media 56, 1–16. http://dx.doi.org/10.1023/B:TIPM.0000018398.19928.5a.
Shi, J., Durucan, S., 2005. A model for changes in coalbed permeability during primary and enhanced methane recovery. SPE Reserv. Eval. Eng. 8 (04), 291–299.
Shi, J.Q., Durucan, S., 2014. Modelling laboratory horizontal stress and coal permeability data using S&D permeability model. Int. J. Coal Geol. 131, 172–176. http://dx.doi.org/10.1016/j.coal.2014.06.014.
Shi, J.-Q., Pan, Z., Durucan, S., 2014. Analytical models for coal permeability changes during coalbed methane recovery: model comparison and performance evaluation. Int. J. Coal Geol. 136, 17–24. http://dx.doi.org/10.1016/j.coal.2014.10.004.
Soeder, D., 1988. Porosity and permeability of eastern Devonian gas shale. SPE Form. Eval. 3, 116–124.
Swami, V., 2012. Shale gas reservoir modeling: from nanopores to laboratory. SPE Annu. Tech. Conf. Exhib. 8–10.
Teufel, L.W., Rhett, D.W., Farrell, H.E., 1991. Effect of Reservoir Depletion and Pore Pressure Drawdown on In Situ Stress and Deformation in the Ekofisk Field, North Sea. 32nd U.S. Symp. Rock Mech, pp. 63–72.
Walls, J., Diaz, E., Cavanaugh, T., 2012. Shale reservoir properties from digital rock physics. Proc. SPE/EAGE Eur. Unconv. Resour. Conf. Exhib. 1–9. http://dx.doi.org/10.2118/152752-MS.
Wang, S., Elsworth, D., Liu, J., 2011. Permeability evolution in fractured coal: the roles of fracture geometry and water-content. Int. J. Coal Geol. 87, 13–25. http://dx.doi.org/10.1016/j.coal.2011.04.009.
Wang, S., Elsworth, D., Liu, J., 2012a. A mechanistic model for permeability evolution in fractured sorbing media. J. Geophys. Res. 117.
Wang, S., Elsworth, D., Liu, J., 2012b. Permeability evolution during progressive deformation of intact coal and implications for instability in underground coal seams. Int. J. Rock Mech. Min. Sci. 1–12.
Wang, G., Ren, T., Wang, K., Zhou, A., 2014. Improved apparent permeability models of gas flow in coal with Klinkenberg effect. Fuel 128, 53–61. http://dx.doi.org/10.1016/j.fuel.2014.02.066.
Yi, J., Akkutlu, I., Deutsch, C., 2008. Gas transport in bidisperse coal particles: investigation for an effective diffusion coefficient in coalbeds. J. Can. Pet. Technol. 47. http://dx.doi.org/10.2118/08-10-20.
Yin, G., Jiang, C., Wang, J.G., Xu, J., 2013. Combined effect of stress, pore pressure and temperature on methane permeability in anthracite coal: an experimental study. Transp. Porous Media 100, 1–16. http://dx.doi.org/10.1007/s11242-013-0202-6.
Zhang, T., Ellis, G.S., Ruppel, S.C., Milliken, K., Yang, R., 2012. Effect of organic-matter type and thermal maturity on methane adsorption in shale-gas systems. Org. Geochem. 47, 120–131. http://dx.doi.org/10.1016/j.orggeochem.2012.03.012.